Electronic Supplementary Material (ESI) for RSC Advances.

Supporting Information

A colorimetric/luminescent benzene compounds sensor based on bis(σ-acetylide) platinum(II) complex: enhancing selectivity and reversibility through dual-recognition sites strategy

Jun Ni,*[a] Jia-Jia Kang,[a] Hui-Hui Wang,[a] Xu-Qiao Gai,[a] Xiao-Xin Zhang,[a] Ting Jia,[a] Liang Xu,[a] Yu-Zhen Pan,[a] and Jian-Jun Zhang*[a]

Chemistry College, Dalian University of Technology, Dalian 116024, China.

Experimental Section

Materials and Reagents. All reactions were carried out under a dry argon atmosphere by using Schlenk techniques and vacuum-line systems unless otherwise specified. The solvents were dried, distilled, and degassed prior to use except that those for spectroscopic measurements were of spectroscopic grade. The ligands 3,8-bis(trimethylsilylethynyl)-1,10-phenanthroline (TMSC≡CPhenC≡CTMS) was prepared as the synthetic procedures described in literature.[1]

Pt(TMSC≡CPhenC≡CTMS)Cl_2. 3,8-bis(trimethylsilylethynyl)-1,10-phenanthroline (37.2 mg, 0.1 mmol) and $Pt(DMSO)_2Cl_2$ (42.2 mg, 0.1 mmol) were added to 50 mL of CH_3CN with stirring for 12 h at ambient temperature. The solvent was removed and the product was purified by column chromatography on silica gel using dichloromethane as eluent. Yield: 81%. ^{1}H NMR (DMSO-d_6, ppm): 0.338 (s, 18H, CH_3), 8.226 (s, 2H, phen), 9.201 (d, 2H, J = 1.6 Hz, phen), 9.479 (d, 2H, J = 1.6 Hz, phen). Anal. Calcd for $C_{22}H_{24}Cl_2N_2PtSi_2$: C, 41.38; H, 3.79; N, 4.39%. Found: C, 41.36; H, 3.77; N, 4.41%. IR (KBr disk, cm^{-1}): 2165m (C≡C), 1252m (Si–C).

Pt(TMSC≡CPhenC≡CTMS)(C≡CPhCl-4)$_2$ (1). $Pt(Me_3SiC{\equiv}CphenC{\equiv}CSiMe_3)Cl_2$ (128 mg, 0.2 mmol), 4-chlorophenylacetylene (60 mg, 0.45 mmol), CuI (1 mg) and diisopropylamine (2 mL) were added to 50 mL of dichloromethane with stirring for 1 d at ambient temperature. The solvent was removed and the product was purified by column chromatography on silica gel using dichloromethane as eluent. Yield: 76%. ^{1}H NMR ($CDCl_3$, ppm): 0.328 (s, 18H, CH_3), 7.238 (d, 4H, J = 8.8 Hz, C_6H_4), 7.515 (d, 4H, J = 8.8 Hz, C_6H_4), 7.924 (s, 2H, phen), 8.600 (s, 2H, phen), 10.023 (s, 2H, phen). Anal. Calcd for $C_{38}H_{32}Cl_2N_2PtSi_2$: C, 54.41; H, 3.85; N, 3.34%. Found: C, 54.39; H, 3.87; N, 3.31%. IR (KBr disk, cm^{-1}): 2165s (C≡C-TMS), 2116m (C≡C-Pt), 1249m (Si–C). ESI-MS (*m/z*): 839 $[M + H]^+$.

Theoretical calculation methodology

Time-dependent density functional theory (DFT/TD-DFT)[2-4] with the gradient-corrected correlation functional PBE1PBE[5] was employed for the calculations. First, the structural geometry of complex **1** as an isolated molecule from the solvent phase in the ground state was optimized at the DFT level of the theory without symmetry constraint. To analyze the spectroscopic properties, 60 singlet and 10 triplet excited states were obtained to determine the vertical excitation energies by performing the TD-DFT calculations on the basis of the optimized geometrical structure. The Stuttgart-Dresden (SDD)[6] basis set consisting of the effective core potentials (ECP) was employed for the platinum(II), and the 6-31G (p, d) polarized double-ζ basis set was used for the remaining non-metal atoms. To precisely describe the electronic structures, one additional *f*-type polarization function was implemented for the platinum(II) atom ($\alpha_f = 0.18$).[7]

As the solvate molecules were found to exert an insignificant influence on the calculated results, a pair of symmetry-related platinum(II) moieties (dimeric model without the solvate molecules) with the shortest intermolecular Pt···Pt distance were used to compare transition characteristics that contribute to the absorption and emission spectra in crystalline species **1**·0.5(CH_2Cl_2) and **1**·0.5(benzene). The Pt-Pt interactions were also estimated by using the Wiberg bond indices (WBIs)[8] with the natural bond orbital (NBO 3.1) program.[9] All calculations were performed with Gaussian 09.[10]

Table S1. Selected atomic distances (Å) and angles (°) of **1**·0.5(CH_2Cl_2) and **1**·0.5(Benzene).

	1·0.5(CH_2Cl_2)	**1**·0.5(Benzene)
Pt···Pt	4.3805(4)	3.5107(6)
Pt···C	1.949(7)	1.941(8)
	1.945(6)	1.939(8)
Pt···N	2.083(4)	2.075(6)
	2.067(6)	2.074(6)
N···Pt···N	80.04(19)	80.5(2)
C···Pt···C	92.5(2)	88.4(3)
N···Pt···C	95.0(2)	95.6(3)
	92.5(2)	95.6(3)

Table S2. Selected hydrogen-bonding geometry (Å,°) and aromatic-ring stacking interaction of **1**·0.5(CH_2Cl_2) and **1**·0.5(benzene).

1·0.5(CH_2Cl_2)					
D-H…*A*	*D*-H	H…*A*	*D*…*A*	*D*-H…*A*	Symmetry code
C1-H1B…Cl1	0.96	2.91	3.786	153	x,3/2-y,-1/2+z
C10-H10…Cl1	0.93	2.93	3.827	161	x,y,-1+z
C11-H11…Cl3’	0.93	2.93	3.609	130	x,y,-1+z
C01’-H01C…π(Cg1)	0.97	2.60	3.565	176	1-x,2-y,1-z
C20-H20C…π(Cg2)	0.96	2.98	3.906	163	2-x,2-y,-z
C21-H21A…π(Cg3)	0.96	2.66	3.602	167	1-x,2-y,-z
C30-H30…Cl3’	0.93	2.89	3.450	120	1-x,2-y,1-z
C34-H34…Cl3	0.93	2.94	3.866	176	1-x,2-y,1-z

Cg1 is the center of bond C23≡C24, Cg2 is the center of bond C4≡C5, Cg3 is the center of benzene ring containing C25 atom.

1·0.5(Benzene)					
D-H…*A*	*D*-H	H…*A*	*D*…*A*	*D*-H…*A*	Symmetry code
C10-H10…π(Cg6)	0.93	2.75	3.655	165	x,1/2-y,1/2+z
C11-H11…π(Cg4)	0.93	2.73	3.633	163	x,1/2-y,1/2+z

	Distance	Symmetry code		Distance	Symmetry code
π(Cg1)…π(Cg2)	3.639	-	π(Cg3)…π(Cg4)	3.392	1-x,1-y,1-z
π(Cg5)…π(Cg6)	3.358	1-x,1-y,1-z			

Cg1 is the center of benzene ring containing C01 atom, Cg2 is benzene ring containing C10 atom, Cg3 is the center of pyridine ring containing N1 atom, Cg4 is the center of bond C31≡C32, Cg5 is the center of pyridine ring containing N2 atom, Cg6 is the center of bond C23≡C24.

Table S3. Partial molecular orbital compositions (%) in the ground state for **1**·0.5(CH_2Cl_2) by TD-DFT method at the PBE1PBE level.

Orbital	Energy (eV)	MO Contribution (%)		
		Pt (s/p/d)	TMSC≡CPhenC≡CTMS	C≡CC_6H_4Cl-4
LUMO+5	-1.22	5.3(3/59/38)	88.4	6.3
LUMO+4	-1.30	6.8(6/68/26)	90.1	3.1
LUMO+3	-2.18	1.3(1/46/53)	97.7	1.0
LUMO+2	-2.21	1.4(35/52/13)	98.0	1.6
LUMO+1	-2.64	3.5(3/33/64)	95.0	1.5
LUMO	-2.65	3.6(18/38/44)	92.9	3.5
HOMO	-5.64	17.3(1/1/98)	1.9	80.8
HOMO-1	-5.66	16.3(1/0/99)	2.1	81.6
HOMO-2	-5.75	21.0(1/3/96)	3.7	75.3
HOMO-3	-5.78	19.3(2/6/92)	4.4	76.3
HOMO-4	-6.13	33.6(2/2/96)	7.7	58.7
HOMO-5	-6.20	33.0(1/3/96)	6.2	60.8
HOMO-6	-6.52	67.7(28/0/72)	7.9	24.4
HOMO-7	-6.60	14.2(6/2/92)	2.7	83.1
HOMO-8	-6.61	32.3(17/1/82)	3.9	63.8
HOMO-9	-6.70	73.7(26/0/74)	21.3	5.0
HOMO-10	-6.94	18.6(25/0/75)	72.8	8.6
HOMO-11	-6.95	4.7(29/1/70)	91.5	3.8
HOMO-12	-7.29	8.6(1/4/95)	27.7	63.7
HOMO-15	-7.35	1.7(9/14/77)	27.5	70.8
HOMO-16	-7.41	20.5(0/1/99)	18.8	60.7

Table S4. Absorption and emission transition properties of **1**·0.5(CH_2Cl_2) by TD-DFT method at the PBE1PBE level with the polarized continuum model (PCM).

States	*E*, nm (eV)	O.S.	Component	Contri.	Assignment	Measured Wavelength (nm)
T_1	574	0.0000	HOMO→LUMO	44%	^{3}MLCT/^{3}LLCT	582
	(2.16)		HOMO-1→LUMO+1	24%	^{3}MLCT/^{3}LLCT	
			HOMO-2→LUMO+1	14%	^{3}MLCT/^{3}LLCT	
T_3	544	0.0000	HOMO-2→LUMO	62%	^{3}MLCT/^{3}LLCT	544
	(2.28)		HOMO→LUMO+1	26%	^{3}MLCT/^{3}LLCT	
S_1	535	0.0143	HOMO→LUMO+1	84%	^{1}MLCT/^{1}LLCT	525
	(2.32)		HOMO-1→LUMO	13%	^{1}MLCT/^{1}LLCT	
S_4	529	0.0087	HOMO-1→LUMO	70%	^{1}MLCT/^{1}LLCT	
	(2.34)		HOMO-2→LUMO	15%	^{1}MLCT/^{1}LLCT	
S_6	511	0.0393	HOMO-2→LUMO	85%	^{1}MLCT/^{1}LLCT	484
	(2.43)		HOMO-1→LUMO	11%	^{1}MLCT/^{1}LLCT	
S_8	503	0.0216	HOMO-3→LUMO+1	87%	^{1}MLCT/^{1}LLCT	
	(2.47)					
S_{10}	454	0.0334	HOMO-4→LUMO+1	54%	^{1}MLCT/^{1}LLCT	453
	(3.59)		HOMO-1→LUMO+2	20%	^{1}MLCT/^{1}LLCT	
			HOMO-5→LUMO	13%	^{1}MLCT/^{1}LLCT	
			HOMO-2→LUMO+2	10%	^{1}MLCT/^{1}LLCT	
S_{12}	448	0.0086	HOMO→LUMO+3	42%	^{1}MLCT/^{1}LLCT	
	(2.77)		HOMO-2→LUMO+2	25%	^{1}MLCT/^{1}LLCT	
			HOMO-1→LUMO+2	15%	^{1}MLCT/^{1}LLCT	
			HOMO-3→LUMO+3	12%	^{1}MLCT/^{1}LLCT	
S_{16}	436	0.0479	HOMO-1→LUMO+2	48%	^{1}MLCT/^{1}LLCT	
	(2.85)		HOMO-2→LUMO+2	22%	^{1}MLCT/^{1}LLCT	
			HOMO-5→LUMO	21%	^{1}MLCT/^{1}LLCT	
			HOMO→LUMO+3	10%	^{1}MLCT/^{1}LLCT	
S_{17}	429	0.0532	HOMO→LUMO+3	44%	^{1}MLCT/^{1}LLCT	429
	(2.89)		HOMO-2→LUMO+2	37%	^{1}MLCT/^{1}LLCT	
S_{20}	420	0.0439	HOMO-3→LUMO+3	63%	^{1}MLCT/^{1}LLCT	
	(2.95)		HOMO-6→LUMO+1	18%	^{1}MLCT/^{1}LLCT	

S_{22}	418	0.0247	HOMO-6→LUMO+1	45%	^{1}MLCT/^{1}LLCT	
	(2.96)		HOMO-3→LUMO+3	22%	^{1}MLCT/^{1}LLCT	
			HOMO-9→LUMO	16%	^{1}IL/^{1}LLCT	
			HOMO-8→LUMO+1	12%	^{1}LLCT	
S_{26}	386	0.0123	HOMO-8→LUMO+1	60%	^{1}LLCT	381
	(3.21)		HOMO-6→LUMO+1	20%	^{1}MLCT/^{1}LLCT	
			HOMO-5→LUMO+2	14%	^{1}MLCT/^{1}LLCT	
S_{28}	382	0.0164	HOMO-7→LUMO	42%	^{1}LLCT/^{1}IL	
	(3.24)		HOMO-4→LUMO+3	30%	^{1}MLCT/^{1}LLCT	
			HOMO-5→LUMO+2	16%	^{1}MLCT/^{1}LLCT	
S_{29}	379	0.0267	HOMO-9→LUMO	40%	^{1}IL/^{1}LLCT	
	(3.27)		HOMO-4→LUMO+3	26%	^{1}MLCT/^{1}LLCT	
			HOMO-5→LUMO+2	18%	^{1}MLCT/^{1}LLCT	
S_{36}	342	0.1037	HOMO-1→LUMO+4	34%	^{1}MLCT/^{1}LLCT	359
	(3.62)		HOMO-10→LUMO	31%	^{1}IL/^{1}LLCT	
			HOMO-7→LUMO+2	10%	^{1}LLCT/^{1}IL	
S_{40}	336	0.0605	HOMO-7→LUMO+2	28%	^{1}LLCT/^{1}IL	337
	(3.69)		HOMO-9→LUMO+2	21%	^{1}IL/^{1}LLCT	
			HOMO-2→LUMO+4	19%	^{1}MLCT/^{1}LLCT	
			HOMO-8→LUMO+3	12%	^{1}IL	
S_{42}	335	0.0221	HOMO-9→LUMO+2	47%	^{1}IL/^{1}LLCT	
	(3.71)		HOMO-8→LUMO+3	27%	^{1}IL	
			HOMO-2→LUMO+4	17%	^{1}MLCT/^{1}LLCT	
S_{44}	333	0.0638	HOMO-10→LUMO	45%	^{1}IL/^{1}LLCT	
	(3.73)		HOMO-1→LUMO+4	19%	^{1}MLCT/^{1}LLCT	
			HOMO-11→LUMO+1	18%	^{1}MLCT/^{1}LLCT	
S_{47}	331	0.1656	HOMO-1→LUMO+4	31%	^{1}MLCT/^{1}LLCT	
	(3.75)		HOMO-11→LUMO+1	30%	^{1}MLCT/^{1}LLCT	
			HOMO-2→LUMO+4	17%	^{1}MLCT/^{1}LLCT	
S_{50}	324	0.6015	HOMO→LUMO+5	41%	^{1}MLCT/^{1}LLCT	
	(3.82)		HOMO-11→LUMO+1	30%	^{1}MLCT/^{1}LLCT	
			HOMO-2→LUMO+4	23%	^{1}MLCT/^{1}LLCT	
S_{52}	321	0.0349	HOMO-10→LUMO+2	28%	^{1}IL/^{1}LLCT	

	(3.86)		HOMO-12→LUMO	19%	^{1}MLCT/^{1}LLCT/^{1}IL	
			HOMO-11→LUMO+2	15%	^{1}MLCT/^{1}LLCT	
			HOMO-15→LUMO+1	13%	^{1}LLCT	
S_{54}	319	0.2054	HOMO-3→LUMO+5	87%	^{1}MLCT/^{1}LLCT	
	(3.89)					
S_{56}	308	0.0379	HOMO-12→LUMO	37%	^{1}MLCT/^{1}LLCT/^{1}IL	307
	(4.03)		HOMO-16→LUMO+1	33%	^{1}IL/^{1}LLCT	
			HOMO-15→LUMO+1	11%	^{1}LLCT	
S_{60}	301	0.0664	HOMO-5→LUMO+4	67%	^{1}MLCT/^{1}LLCT	
	(4.12)		HOMO-4→LUMO+5	27%	^{1}MLCT/^{1}LLCT	

Table S5. Partial molecular orbital compositions (%) in the ground state for **1**·0.5(Benzene) by TD-DFT method at the PBE1PBE level.

Orbital	Energy (eV)	MO Contribution (%)		
		Pt (s/p/d)	TMSC≡CPhenC≡CTMS	C≡CC_6H_4Cl-4
LUMO+5	-1.01	4.2(39/46/15)	87.3	8.6
LUMO+4	-1.32	9.0(28/61/11)	84.5	6.5
LUMO+3	-2.00	0.9(2/78/20)	98.3	0.8
LUMO+2	-2.09	1.3(2/26/72)	97.0	1.7
LUMO+1	-2.61	2.2(40/29/31)	94.8	3.0
LUMO	-2.65	4.2(10/39/51)	93.1	2.7
HOMO	-5.57	22.5(0/6/94)	2.5	75.0
HOMO-1	-5.69	24.1(8/2/90)	3.0	72.9
HOMO-2	-5.75	38.2(15/2/83)	4.4	57.4
HOMO-3	-5.76	25.0(3/6/91)	4.6	70.4
HOMO-4	-6.16	65.9(23/2/75)	5.0	29.1
HOMO-5	-6.22	38.2(6/1/93)	3.1	58.7
HOMO-6	-6.22	30.9(1/1/98)	2.1	67.0
HOMO-7	-6.62	3.3(0/24/76)	13.3	83.4
HOMO-8	-6.64	3.5(0/23/77)	6.2	90.3
HOMO-9	-6.88	7.0(0/0/100)	78.7	14.3
HOMO-10	-6.99	0.7(17/38/45)	87.2	12.1
HOMO-11	-7.14	72.6(27/0/73)	3.6	23.7
HOMO-12	-7.15	10.5(2/1/97)	20.7	68.8
HOMO-13	-7.23	20.7(22/1/77)	3.3	76.0
HOMO-14	-7.28	3.5(0/1/99)	12.1	84.4
HOMO-15	-7.30	6.0(19/4/77)	4.4	89.6
HOMO-16	-7.40	7.2(2/2/96)	24.4	68.4

Table S6. Absorption and emission transition properties of **1**·0.5(Benzene) by TD-DFT method at the PBE1PBE level with the polarized continuum model (PCM).

States	*E*, nm (eV)	O.S.	Component	Contri.	Assignment	Measured Wavelength (nm)
T_1	594	0.0000	HOMO→LUMO	90%	^{3}MLCT/^{3}MLCT	638
	(2.09)					
S_3	542	0.0128	HOMO-2→LUMO	49%	^{1}MLCT/^{1}LLCT	542
	(2.23)		HOMO-1→LUMO	31%	^{1}MLCT/^{1}LLCT	
			HOMO-3→LUMO+1	10%	^{1}MLCT/^{1}LLCT	
S_8	497	0.1103	HOMO-3→LUMO+1	90%	^{1}MLCT/^{1}LLCT	508
	(2.49)					
S_9	460	0.0325	HOMO-4→LUMO	73%	^{1}MLCT/^{1}LLCT	461
	(2.69)		HOMO→LUMO+2	17%	^{1}MLCT/^{1}LLCT	
S_{13}	445	0.0746	HOMO→LUMO+2	69%	^{1}MLCT/^{1}LLCT	
	(2.79)		HOMO-4→LUMO	16%	^{1}MLCT/^{1}LLCT	
S_{16}	437	0.0101	HOMO-6→LUMO+1	97%	^{1}MLCT/^{1}LLCT	435
	(3.22)					
S_{18}	423	0.0095	HOMO-3→LUMO+2	61%	^{1}MLCT/^{1}LLCT	423
	(2.93)		HOMO-2→LUMO+3	25%	^{1}MLCT/^{1}LLCT	
			HOMO-1→LUMO+3	14%	^{1}MLCT/^{1}LLCT	
S_{20}	412	0.0136	HOMO-3→LUMO+2	41%	^{1}MLCT/^{1}LLCT	409
	(3.01)		HOMO-1→LUMO+3	33%	^{1}MLCT/^{1}LLCT	
			HOMO-2→LUMO+3	26%	^{1}MLCT/^{1}LLCT	
S_{21}	407	0.0468	HOMO-2→LUMO+3	50%	^{1}MLCT/^{1}LLCT	
	(3.04)		HOMO-1→LUMO+3	45%	^{1}MLCT/^{1}LLCT	
S_{24}	386	0.0240	HOMO-8→LUMO	71%	^{1}LLCT	383
	(3.21)		HOMO-7→LUMO+1	25%	^{1}LLCT/^{1}IL	
S_{26}	375	0.0102	HOMO-7→LUMO+1	74%	^{1}LLCT/^{1}IL	365
	(3.30)		HOMO-8→LUMO	26%	^{1}LLCT	
S_{34}	345	0.0940	HOMO-1→LUMO+4	61%	^{1}MLCT/^{1}LLCT	344
	(3.59)		HOMO-9→LUMO	39%	^{1}IL/^{1}LLCT	
S_{36}	343	0.1046	HOMO-2→LUMO+4	64%	^{1}MLCT/^{1}LLCT	
	(3.61)		HOMO-9→LUMO	16%	^{1}IL/^{1}LLCT	

			HOMO-11→LUMO+1	13%	^{1}MLCT/^{1}LLCT	
S_{38}	337	0.0147	HOMO-11→LUMO+1	70%	^{1}MLCT/^{1}LLCT	330
	(3.68)		HOMO-13→LUMO+1	11%	^{1}MLCT/^{1}LLCT	
S_{40}	334	0.2103	HOMO-9→LUMO	38%	^{1}IL/^{1}LLCT	
	(3.71)		HOMO-1→LUMO+4	32%	^{1}MLCT/^{1}LLCT	
			HOMO-2→LUMO+4	25%	^{1}MLCT/^{1}LLCT	
S_{44}	326	0.0611	HOMO→LUMO+5	50%	^{1}MLCT/^{1}LLCT	
	(3.80)		HOMO-10→LUMO+1	45%	^{1}IL/^{1}LLCT	
S_{45}	319	0.0160	HOMO-12→LUMO	62%	^{1}MLCT/^{1}LLCT/^{1}IL	
	(4.13)					
S_{47}	318	0.7241	HOMO-10→LUMO+1	50%	^{1}IL/^{1}LLCT	316
	(3.90)		HOMO→LUMO+5	47%	^{1}MLCT/^{1}LLCT	
S_{51}	314	0.0665	HOMO-13→LUMO+1	26%	^{1}MLCT/^{1}LLCT	
	(3.95)		HOMO-12→LUMO	20%	^{1}MLCT/^{1}LLCT/^{1}IL	
			HOMO-14→LUMO	10%	^{1}IL/^{1}LLCT	
			HOMO-16→LUMO	9%	^{1}IL/^{1}LLCT	
S_{54}	309	0.1078	HOMO-4→LUMO+4	42%	^{1}MLCT/^{1}LLCT	308
	(4.02)		HOMO-14→LUMO	32%	^{1}IL/^{1}LLCT	
			HOMO-13→LUMO	10%	^{1}MLCT/^{1}LLCT	
S_{56}	307	0.0775	HOMO-3→LUMO+5	65%	^{1}MLCT/^{1}LLCT	
	(4.04)		HOMO-5→LUMO+4	22%	^{1}MLCT/^{1}LLCT	
			HOMO-4→LUMO+4	10%	^{1}MLCT/^{1}LLCT	
S_{57}	306	0.0669	HOMO-4→LUMO+4	38%	^{1}MLCT/^{1}LLCT	
	(4.04)		HOMO-14→LUMO	26%	^{1}IL/^{1}LLCT	
			HOMO-15→LUMO+1	22%	^{1}LLCT	
			HOMO-16→LUMO	11%	^{1}IL/^{1}LLCT	
S_{59}	304	0.0523	HOMO-5→LUMO+4	68%	^{1}MLCT/^{1}LLCT	
	(4.08)		HOMO-3→LUMO+5	21%	^{1}MLCT/^{1}LLCT	

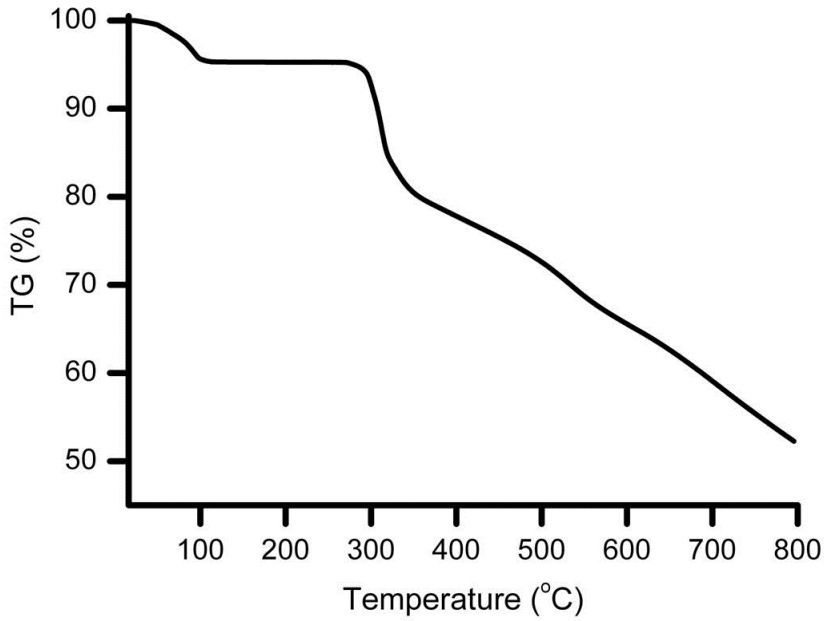

Figure S1. Thermal gravitational (TG) curve for **1**·0.5(CH_2Cl_2) showing weight loss of solvate CH_2Cl_2 at 60-100°C and decomposition temperature above 280°C.

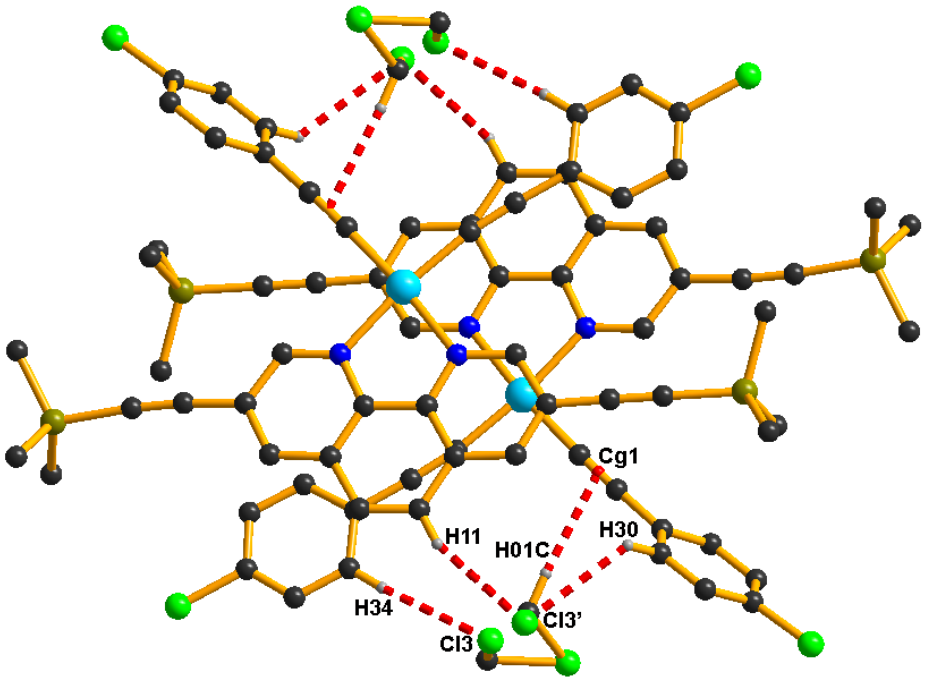

Figure S2. Crystal packing diagram of planar platinum(II) moieties in **1**·0.5(CH_2Cl_2), showing C-H…Cl and C-H…π hydrogen bond between solvate CH_2Cl_2 molecule and platinum moieties.

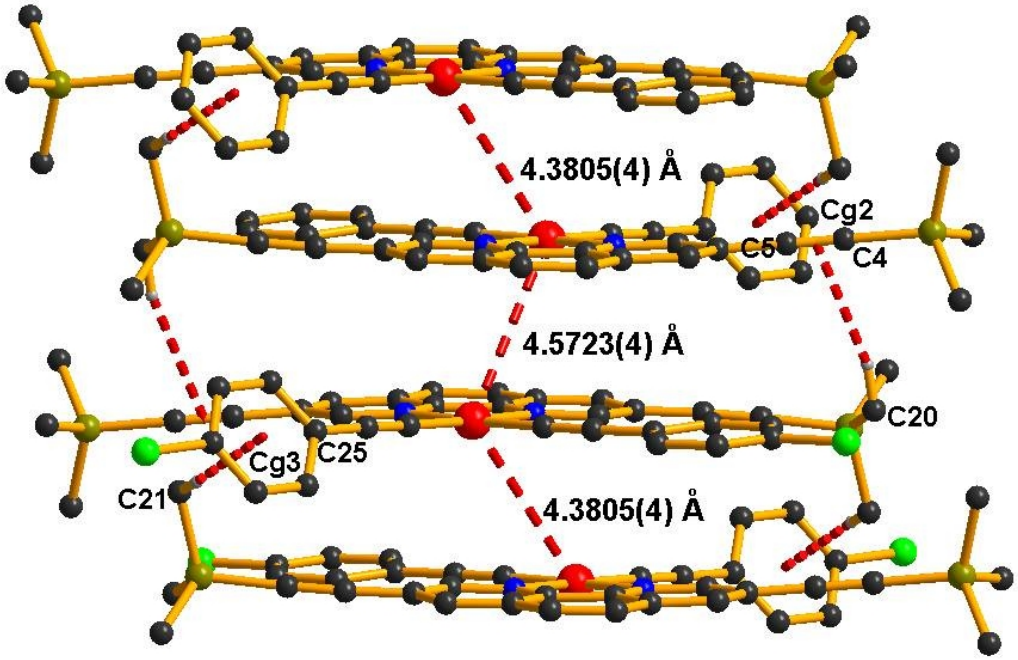

Figure S3. Crystal packing diagram of planar platinum(II) moieties in **1**·0.5(CH_2Cl_2), showing C-H…π hydrogen bond between adjacent platinum moieties.

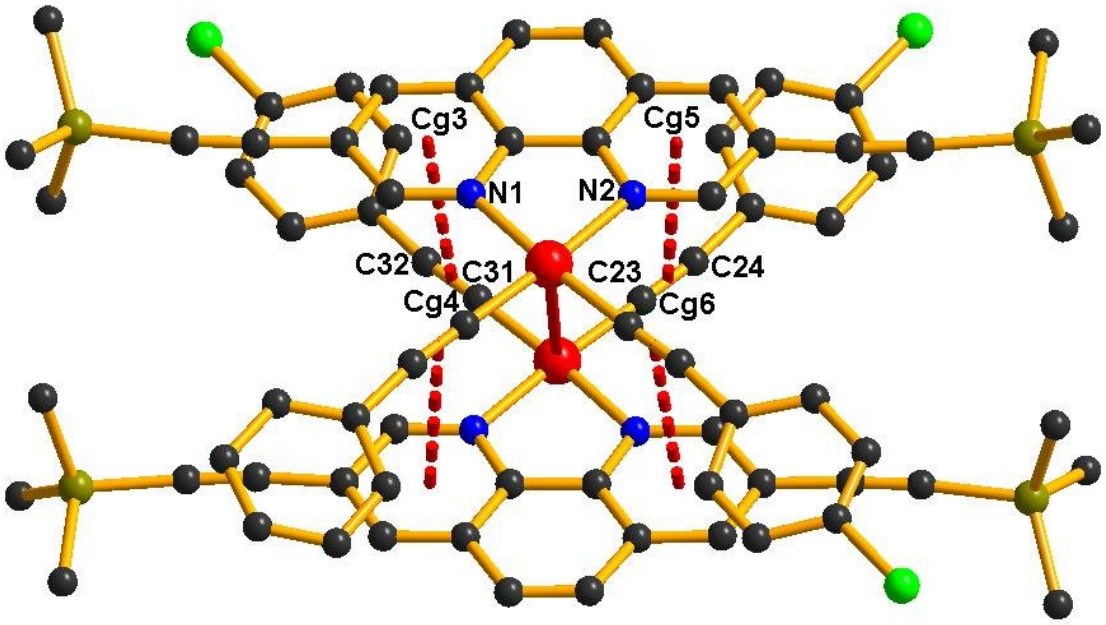

Figure S4. Crystal packing diagram of planar platinum(II) moieties in **1**·0.5(Benzene), showing aromatic-ring π···π stacking interaction between adjacent platinum moieties.

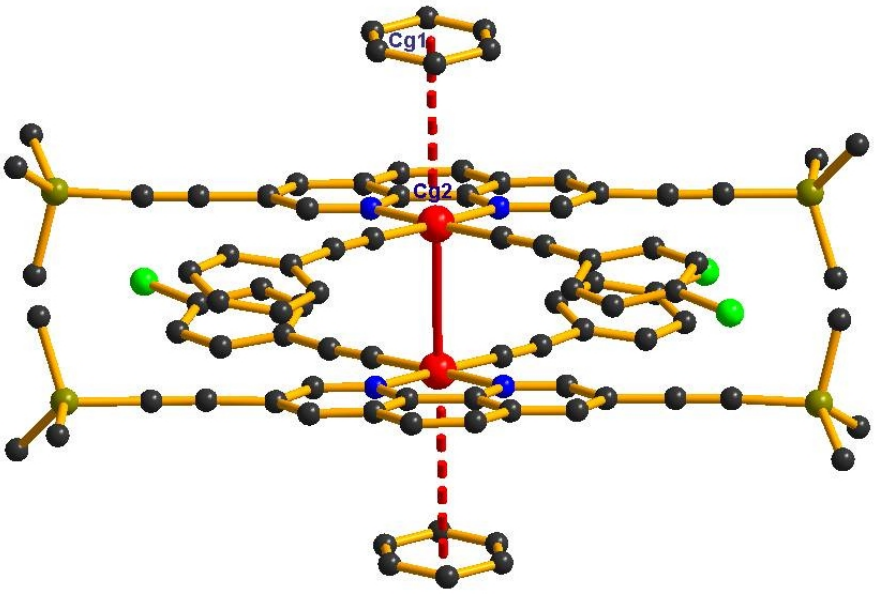

Figure S5. Crystal packing diagram of planar platinum(II) moieties in **1**·0.5(Benzene), showing aromatic-ring π···π stacking interaction between solvate benzene molecule and platinum moieties.

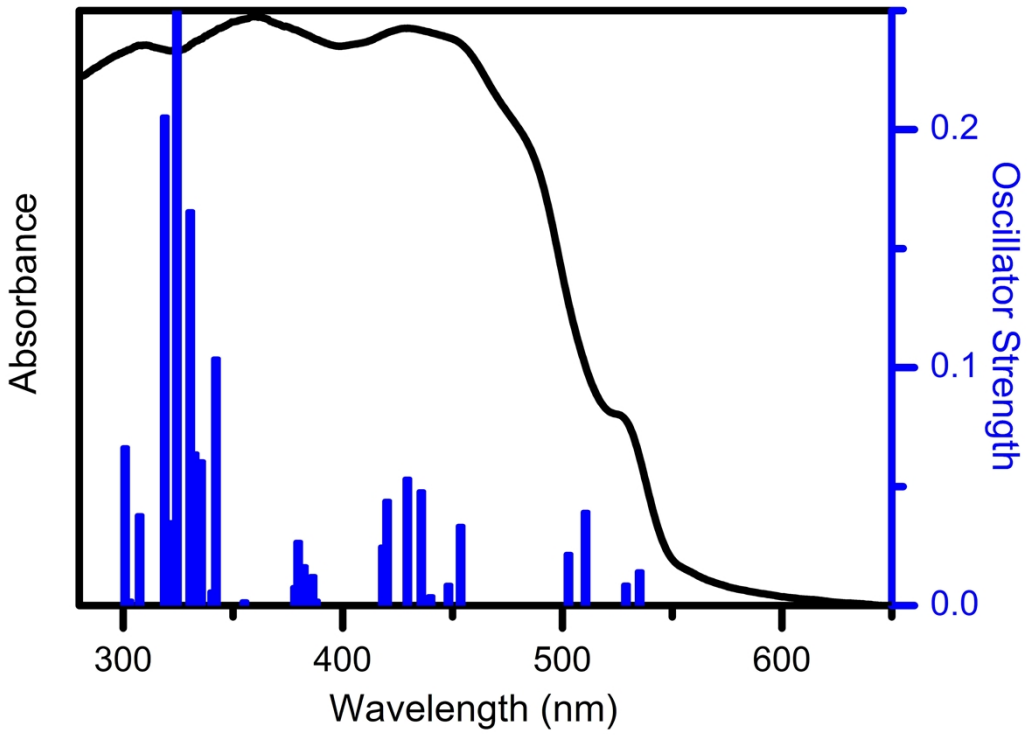

Figure S6. Calculated (blue vertical bars) and measured (black line) UV-Vis absorption spectra of solid-state **1**·0.5(CH_2Cl_2) at ambient temperature.

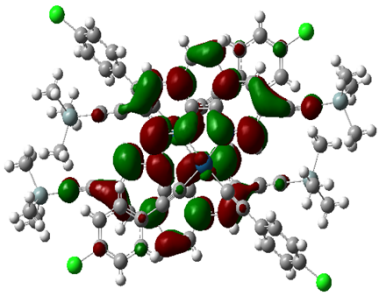

LUMO+5

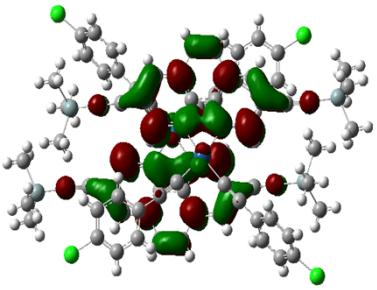

LUMO+4

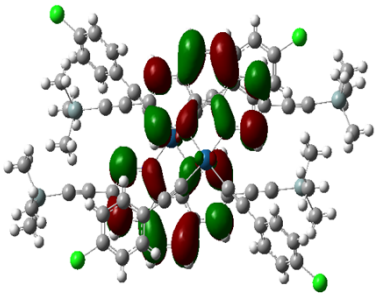

LUMO+3

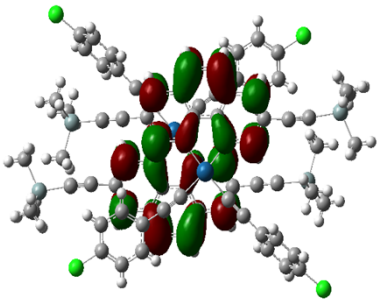

LUMO+2

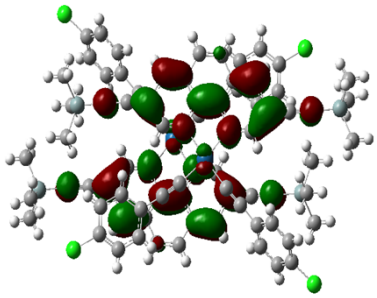

LUMO+1

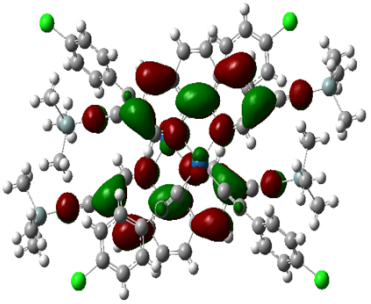

LUMO

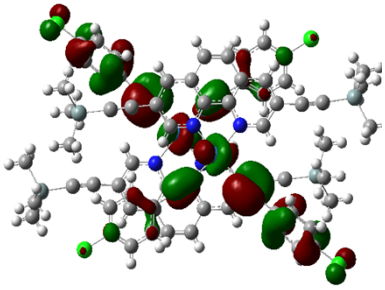

HOMO

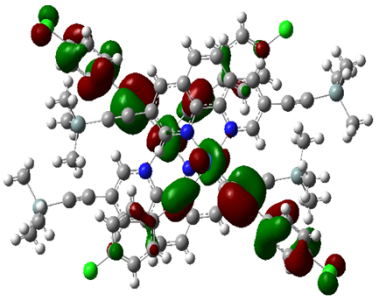

HOMO-1

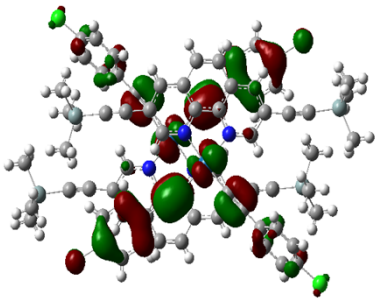

HOMO-2

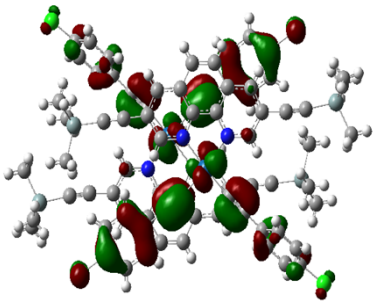

HOMO-3

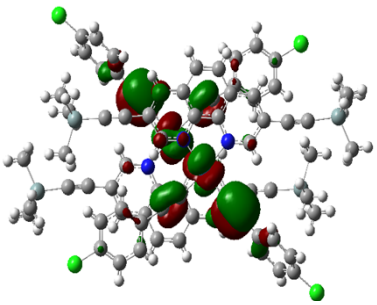

HOMO-4

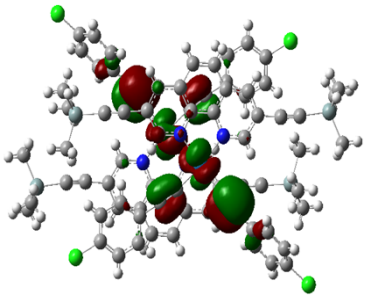

HOMO-5

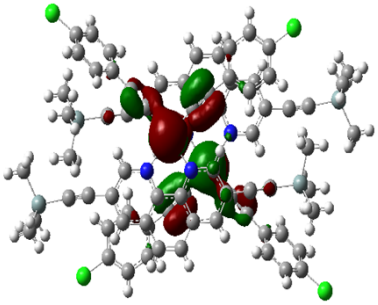

HOMO-6

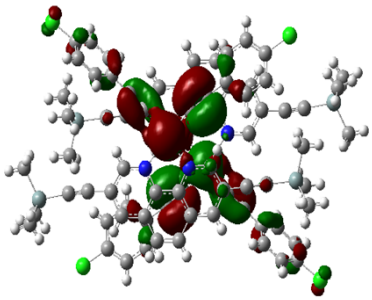

HOMO-7

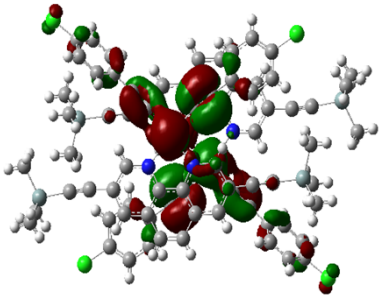

HOMO-8

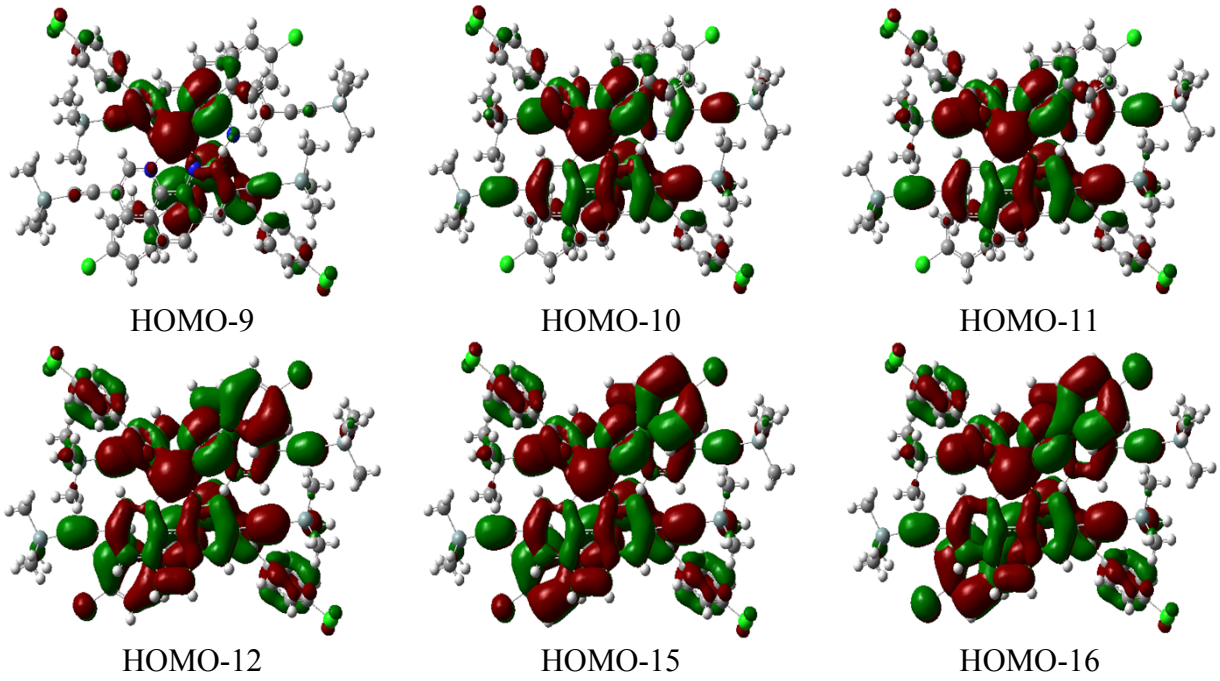

Figure S7. Plots of the frontier molecular orbitals involved in the absorption of **1**·0.5(CH_2Cl_2) in solid state (isovalue = 0.02).

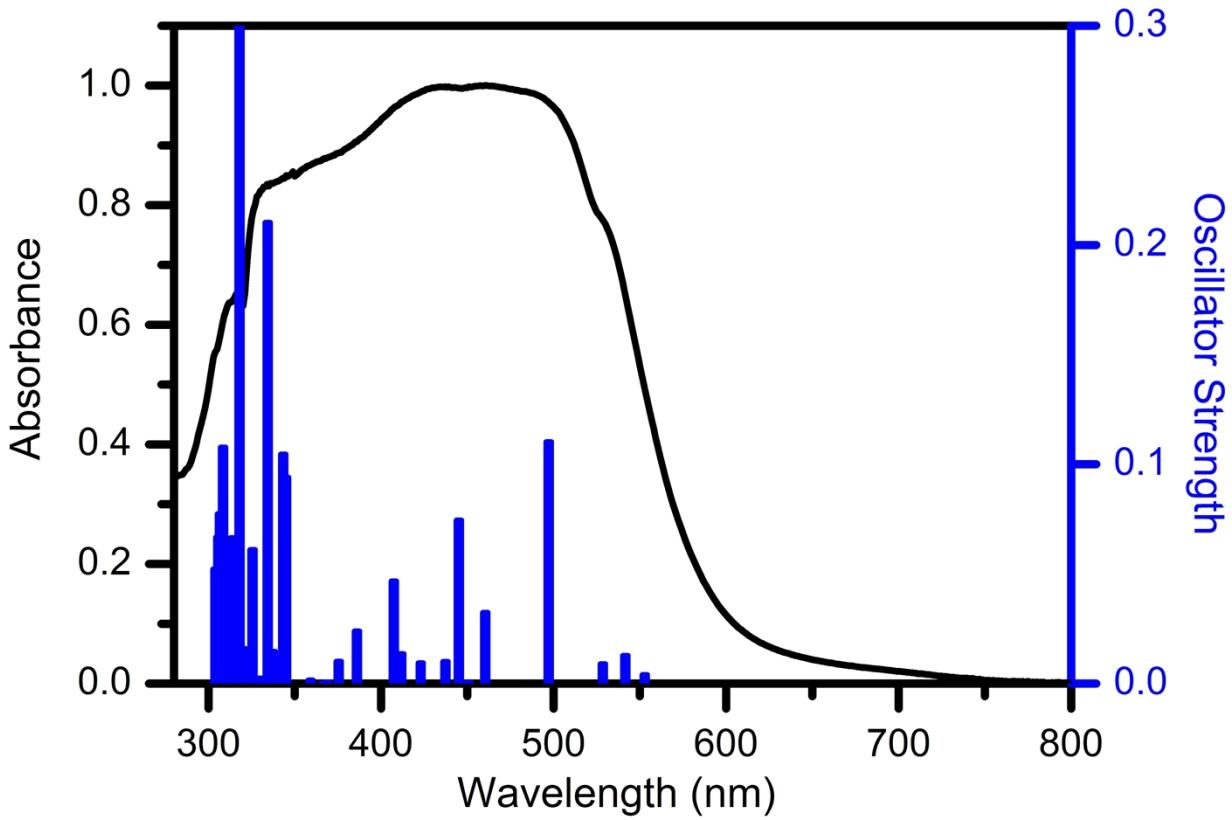

Figure S8. Calculated (blue vertical bars) and measured (black line) UV-Vis absorption spectra of solid-state **1**·0.5(Benzene) at ambient temperature.

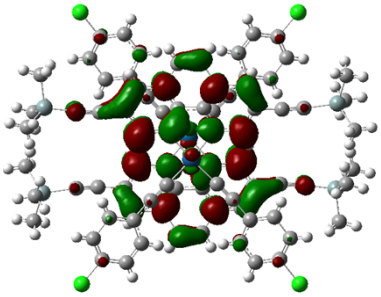

LUMO+5

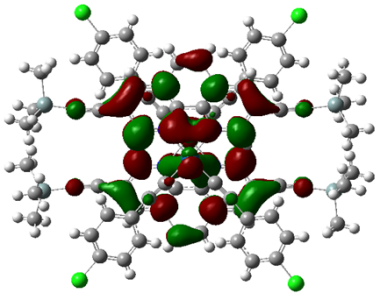

LUMO+4

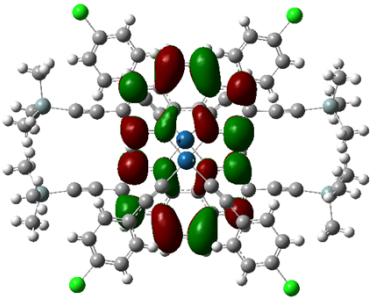

LUMO+3

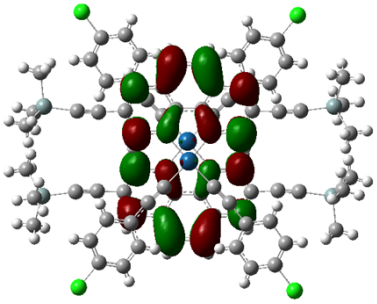

LUMO+2

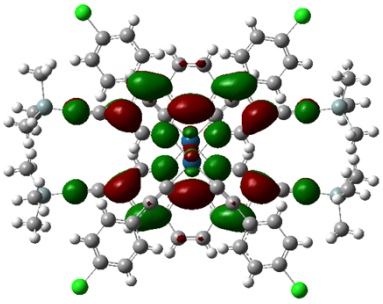

LUMO+1

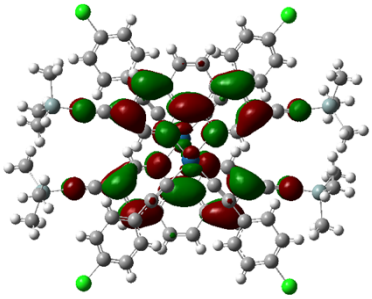

LUMO

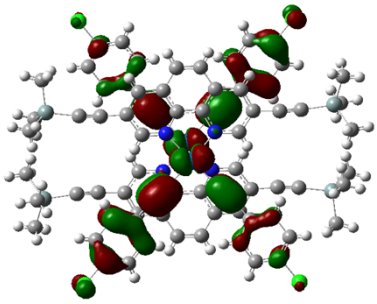

HOMO

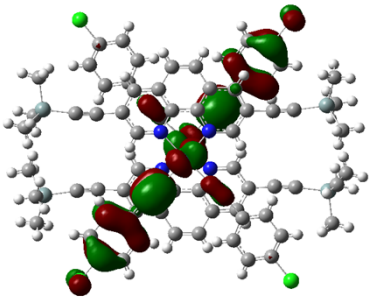

HOMO-1

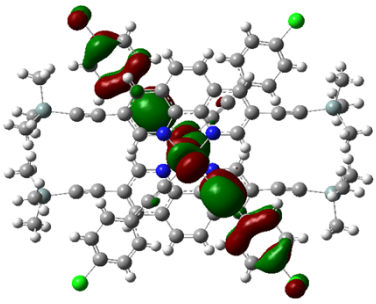

HOMO-2

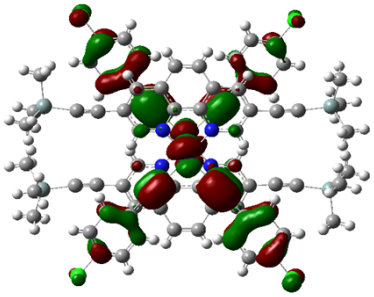

HOMO-3

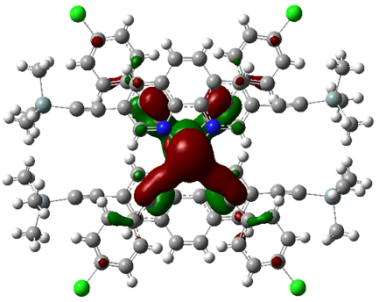

HOMO-4

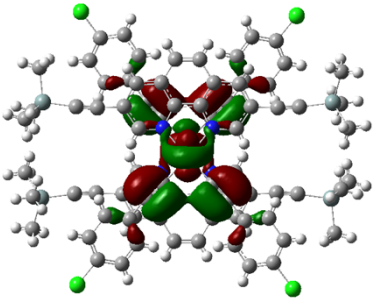

HOMO-5

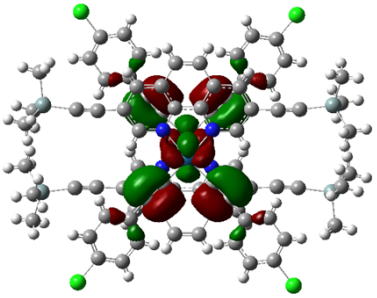

HOMO-6

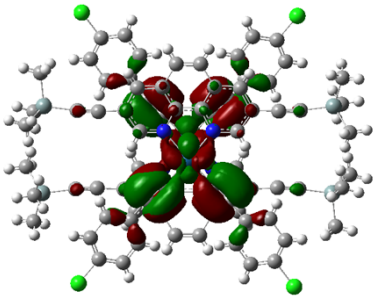

HOMO-7

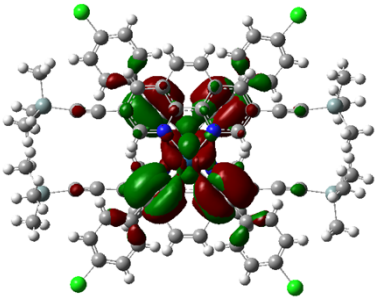

HOMO-8

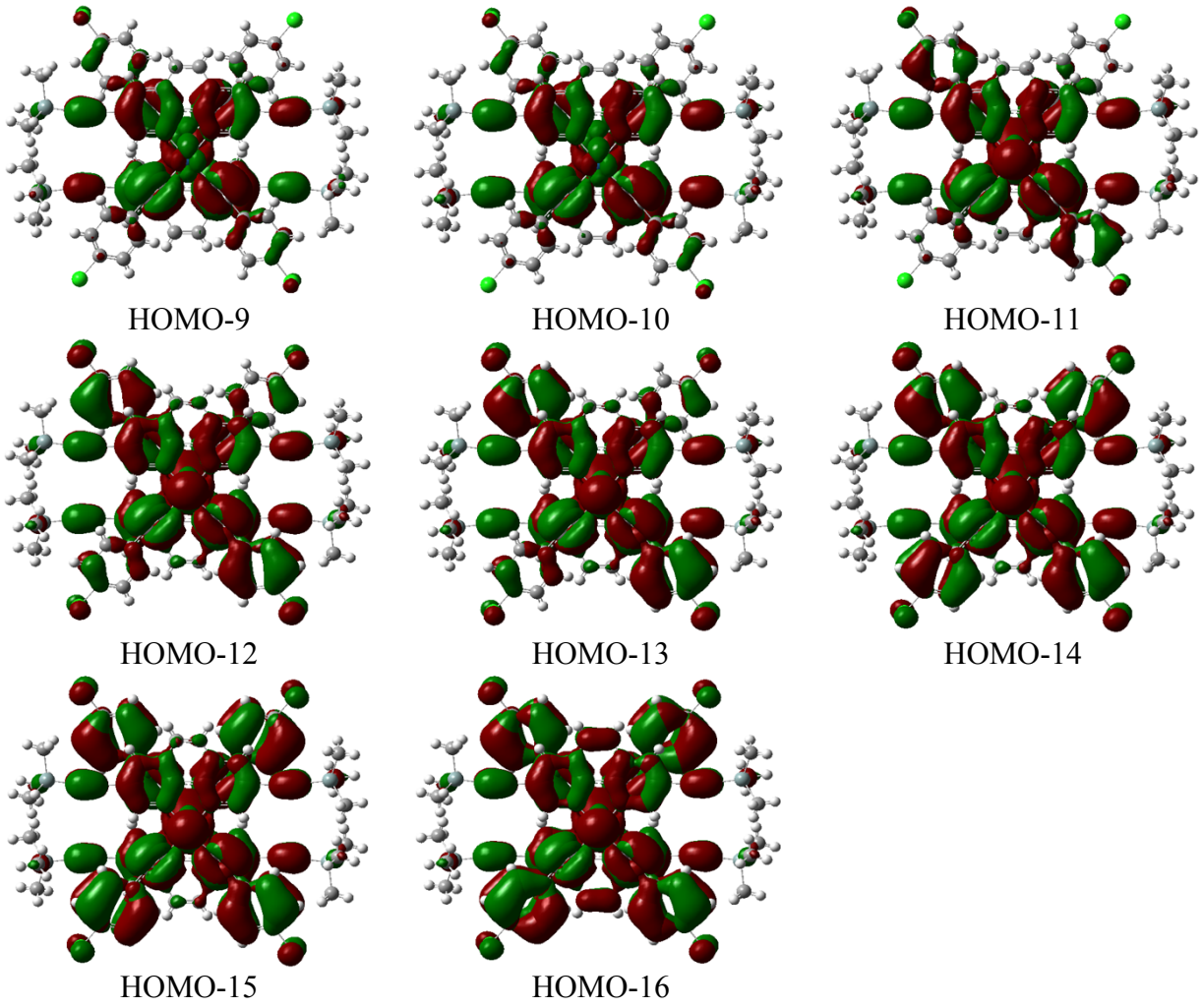

Figure S9. Plots of the frontier molecular orbitals involved in the absorption of **1**·0.5(Benzene) in solid state (isovalue = 0.02).

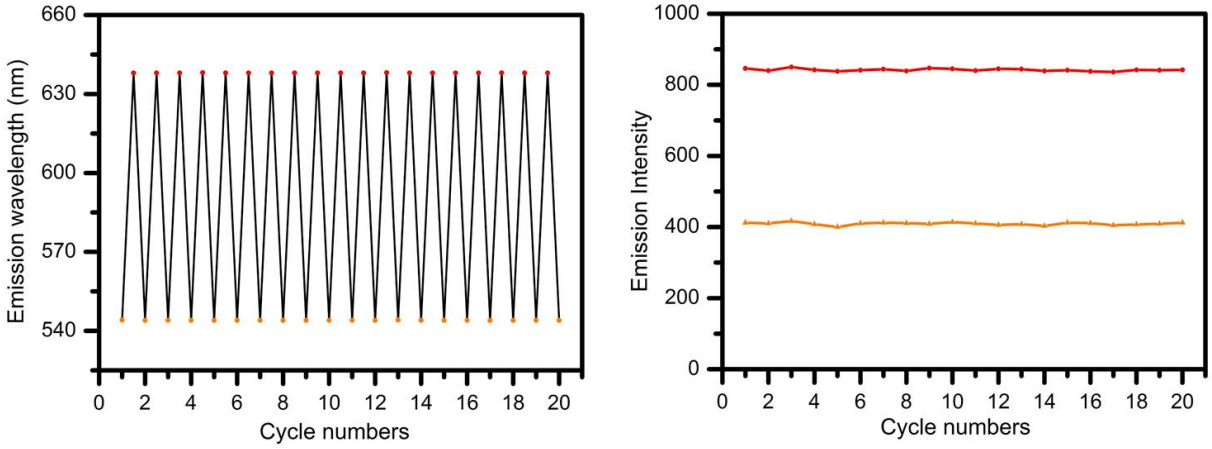

Figure S10. Changes of the emission wavelength (left) and intensity (right) in the reversible vapochromic cycles **1**·0.5(CH_2Cl_2) ⇌ **1**·0.5(Benzene), beginning with **1**·0.5(CH_2Cl_2).

References

1. R. Ziessel and C. Stroh, *Tetrahedron Lett.*, 2004, **45**, 4051.
2. A. D. Becke, *J. Chem. Phys.*, 1993, **98**, 5648.
3. M. E. Casida, C. Jamorski, K. C. Casida and D. R. Salahub, *J. Chem. Phys.*, 1998, **108**, 4439.
4. R. E. Stratmann, G. E. Scuseria and M. J. Frisch, *J. Chem. Phys.*, 1998, **109**, 8218.
5. J. P. Perdew, K. Burke and M. Ernzerhof, *Phys. Rev. Lett.*, 1996, **77**, 3865.
6. (a) D. Andrae, U. Haussermann, M. Dolg, H. Stoll and H. Preuss, *Theor. Chim. Acta*, 1990, **77**, 123; (b) P. Schwerdtfeger, M. Dolg, W. H. E. Schwarz, G. A. Bowmaker and P. D. W. Boyd, *J. Chem. Phys*., 1989, **91**, 1762; (c) M. Dolg, U. Wedig, H. Stoll and H. Preuss, *J. Chem. Phys.*, 1987, **86**, 866.
7. (a) P. Pyykkö, N. Runeberg and F. Mendizabal, *Chem. Eur. J.*, 1997, **3**, 1451; (b) P. Pyykkö and F. Mendizabal, *Chem. Eur. J.*, 1997, **3**, 1458.
8. C. M. Breneman and K. B. Wiberg, *J. Comput. Chem.*, 1990, **11**, 361.
9. *NBO Version 3.1*, E. D. Glendening, J. K. Badenhoop, A. E. Reed, J. E. Carpenter, F. Weinhold, Theoretical Chemistry Institute, University of Wisconsin, Madison.
10. M. J. Frisch, G. W. Trucks, H. B. Schlegel, G. E. Scuseria, M. A. Robb, J. R. Cheeseman, G. Scalmani, V. Barone, B. Mennucci, G. A. Petersson, H. Nakatsuji, M. Caricato, X. Li, H. P. Hratchian, A. F. Izmaylov, J. Bloino, G. Zheng, J. L. Sonnenberg, M. Hada, M. Ehara, K. Toyota, R. Fukuda, J. Hasegawa, M. Ishida, T. Nakajima, Y. Honda, O. Kitao, H. Nakai, T.

Vreven, J. A. Montgomery, Jr., J. E. Peralta, F. Ogliaro, M. Bearpark, J. J. Heyd, E. Brothers, K. N. Kudin, V. N. Staroverov, R. Kobayashi, J. Normand, K. Raghavachari, A. Rendell, J. C. Burant, S. S. Iyengar, J. Tomasi, M. Cossi, N. Rega, J. M. Millam, M. Klene, J. E. Knox, J. B. Cross, V. Bakken, C. Adamo, J. Jaramillo, R. Gomperts, R. E. Stratmann, O. Yazyev, A. J. Austin, R. Cammi, C. Pomelli, J. W. Ochterski, R. L. Martin, K. Morokuma, V. G. Zakrzewski, G. A. Voth, P. Salvador, J. J. Dannenberg, S. Dapprich, A. D. Daniels, O. Farkas, J. B. Foresman, J. V. Ortiz, J. Cioslowski, D. J. Fox, Gaussian 09, Revision A.01, Gaussian, Inc., Wallingford, CT, **2009**.